

Luminosity measurement method for the LHC: The detector requirements studies*

M. W. Krasny^a, J. Chwastowski^{b c}, A. Cyz^c and K. Słowikowski^c

^a LPNHE, Pierre and Marie Curie University, CNRS-IN2P3, Tour 33, RdC, 4, pl. Jussieu, 75005 Paris, France.

^b Institute of Teleinformatics, Faculty of Physics, Mathematics and Computer Science, Cracow University of Technology, ul. Warszawska 24, 31-115 Kraków, Poland.

^c Institute of Nuclear Physics PAN, ul. Radzikowskiego 152, 31-342 Kraków, Poland.

Absolute normalisation of the LHC measurements with a precision of $\mathcal{O}(1\%)$ is desirable but beyond the reach of the present LHC detectors. This series of papers proposes and evaluates a measurement method capable to achieve such a precision target. In our earlier paper [1] we have selected the phase-space region where the lepton pair production cross section in pp collisions at the LHC can be controlled with $\leq 1\%$ precision and is large enough to reach a comparable statistical accuracy of the absolute luminosity measurement on the day-by-day basis. In the present one the performance requirements for a dedicated detector, indispensable to efficiently select events in the proposed phase-space region, are discussed.

1. Introduction

For the direct searches for new particles at the LHC the precision of the absolute normalisation of the measured cross sections is of secondary importance. However, to fully exploit the LHC discovery potential, direct searches must be complemented by precise measurements of the Standard Model cross sections and, subsequently, by the scrutiny of their compatibility with those determined at the previous colliders. Achieving the highest possible precision of the absolute scale of the LHC cross sections is of utmost importance for such a complementary programme.

Presently, no viable measurement scheme capable to reach the desired $\leq 1\%$ precision of the absolute scale of the cross sections exists. Moreover, no scheme exists allowing to

*This work was supported in part by the programme of co-operation between the IN2P3 and Polish Laboratories No. 05-117, Polonium Programme No. 17783NY and Polish Grant No. 665/N-CERN-ATLAS/2010/0.

cross-normalise the LHC cross sections measured at variable centre-of-mass energies and variable LHC beam particle species (ions) to a desirable precision level of $\leq 0.1\%$.

This paper is the second one of the series of papers presenting a measurement method which is capable of achieving the above precision goals. This method is based on the measurement of the rate of the opposite-charge lepton pairs produced in peripheral collisions of the beams' particles.

In [1] we have selected the kinematic region in which the rate is large enough to reach a 1% statistical precision of the luminosity measurement on the day-by-day basis. We have demonstrated that better than 1% accuracy of the theoretical control of the pair rate can be reached by a restriction of their allowed phase-space to the region of small transverse momentum leptons produced back-to-back in the plane transverse to the collision axis. Such a restriction allowed us to suppress drastically the contribution of the inelastic collisions and those of elastic collisions in which the internal charge structure of protons is resolved.

Efficient selection of electromagnetically produced lepton pairs in the proposed phase-space region, out of a huge background of any unlike charge particle pairs produced in the ordinary, minimum bias collisions of the LHC beam particles, represents a major challenge. For the bunched beams, colliding at large luminosity the challenge is twofold. The overall rejection power of the background hadron pairs of the order of $\sim 10^{10}$ must be achieved. However, the most difficult challenge is to drastically reduce the GHz-range rate of the background pairs at the very early stage of the data selection process – preferentially at the first trigger level (LVL1). This is obviously beyond the reach of the present general purpose LHC detectors.

Our most important constraint for designing a luminosity detector which allows to meet the above requirements is that it should be fully incorporated within the fiducial volume of one of the already existing LHC detectors. In particular, its trigger and the data acquisition (TDAQ) system should be a partition of the host detector TDAQ. The rationale behind such a constraint is twofold. Firstly, the host detector signals will play an important role in the overall background rejection scheme, both for the high level trigger (HLT) and the off-line selection stages. Secondly, the host-detector offline reconstructed objects could be used for precise monitoring of the luminosity detector performance. The luminosity events, once accepted by the luminosity detector LVL1 trigger, could be exposed to the host detector specific event selection procedures in the same way as all the other events. Owing to such a scheme, the dead time corrected luminosity can be directly measured².

For the studies of the luminosity detector performance requirements, presented in this paper, we have chosen ATLAS [2] as the host detector. This detector, following the decision of the ATLAS collaboration to stage the production of the TRT C-wheels, disposes an empty space which could, in principle, accommodate the luminosity detector. This leftover space happens to be the most optimal one for a detector satisfying all the

² Only in such a case the precision of the measured rate of the lepton pairs could be directly reflected in the precision of the absolute normalisation of any event sample, regardless of the time variation of: the bunch-by-bunch beam intensity, the time dependent detector operation efficiency, and the TDAQ dead time.

requirements discussed in this paper³.

The paper is organised as follows. In section 2 the general aspects of the event selection strategy are presented. The tools and the simulation methods are discussed in section 3. In section 4 the luminosity detector geometry and the magnetic field configurations are introduced. The characteristics of the background and the signal events are presented in section 5. Section 6 is devoted to the detector resolution requirements discussion. The dead material effects are evaluated in section 7. Finally, section 8 is focussed on the trigger and the data acquisition system requirements.

2. An initial overview of the event selection strategy

In our previous paper [1], an optimal phase-space region of the lepton pair production process $pp \rightarrow l^+l^- + X$, for the LHC luminosity measurement was selected. Our choice was driven by the following two requirements:

- to assure a high rate of the corresponding "luminosity" events,
- to guarantee a high precision of its theoretical control,

while taking into account the real constraints of the existing general-purpose LHC experiments. The optimal compromise was achieved by requesting leptons to be produced in the central pseudorapidity region, $-2.7 \leq \eta \leq 2.7$. Their transverse momenta were requested to satisfy the conditions: $p_T^{l^+}, p_T^{l^-} \geq 0.1 \text{ GeV}/c$.

The ATLAS detector has the requisite capacity to measure both the tracks and the calorimetric energy deposits of such leptons. However, in its present configuration it is unable to select on-line a requisite fraction of events with leptons in the selected phase-space region. Such a task is difficult because lepton pairs, produced in the selected kinematic region, represent a 10^{-9} fraction of all the unlike charge hadron pairs produced in ordinary minimum-bias hadron processes.

The detector upgrade requirements are thus driven by the necessity of adding the triggering capacity for the luminosity events. Variety of triggering strategies could be employed. Each of them would lead to a different requirements for the detector upgrade. The selection strategy advocated below minimises the interference with the host detector layout and its TDAQ architecture. More importantly, it minimises the usage of the host detector TDAQ resources to a level which will hardly be noticeable.

The ATLAS LVL1 trigger can accept events with maximum frequency of 100 kHz [3]. It is assumed that of the order of 1% of this bandwidth could be assigned to the lepton pair production candidates. In such a case the initial rate of the charged hadron pairs has to be reduced by a factor of 10^7 already by the LVL1 trigger. The above rate reduction has to be based, almost exclusively, on the trigger signals coming from the dedicated luminosity detector. Once the initial rate of the lepton pair candidate events is reduced to a 1 kHz level a further selection of events by the level 2 trigger (LVL2) and by the event filter (EF), can be based entirely on the ATLAS detector signals. As a consequence the performance requirements for a dedicated luminosity detector will be specified, almost exclusively, in terms of its LVL1 triggering capacity.

³The dead material budget of such a detector could be smaller than that of the TRT C-wheels and its presence would not deteriorate the performance quality of the ATLAS detector.

Several event-selection strategies based on the pair-by-pair rejection principle were investigated. None of them was able to satisfy the LVL1 latency requirement. Therefore, compromises had to be made.

A strategy capable of achieving such a rejection factor must drastically reduce the rate of the bunch crossings which will be fully analysed by the luminosity detector LVL1 trigger logic. Moreover, the analysed bunch crossings must have a significantly smaller multiplicity of charged particles traversing the fiducial volume of the luminosity detector than the rejected bunch crossings.

In [1] we proposed to select only the “silent bunch crossings” for the luminosity determination. A “silent bunch crossing” was defined as a bunch crossing in which none of the protons of the colliding bunches had a strong interaction mediated collision. In this paper, the above definition will be reformulated using the using solely the LVL1 signals of the luminosity detector⁴.

The necessity of the initial reduction of the rate of the fully analysed bunch crossings excludes a direct applicability of the proposed method over the periods of the machine operation in which the delivered luminosity will be higher than $L \sim 3 \times 10^{33} \text{ cm}^{-2} \text{ s}^{-1}$ (if the luminosity is distributed uniformly among the colliding bunches). The luminosity collected in such machine operation periods will be determined by a complementary method⁵.

An important singularity of our event selection strategy is the choice of events, containing a pair of particles with highly collinear, back-to-back transverse momenta, already by the luminosity detector LVL1 trigger logic. Lepton identification is left to the subsequent trigger levels. The rationale behind such a choice is that only the rate of such a subsample of events can be controlled theoretically with satisfactory precision [1]. The LVL1 selected sample is dominated by the charged hadron pairs produced in the ordinary minimum bias processes. This background can be determined experimentally to a very high precision because minimum bias events are recorded parasitically in all the phases of the detector operation, providing the requisite background monitoring data samples. The background subtraction scheme will thus be based entirely on the collected data and will be independent of all the modelling aspects of the soft hadron interactions.

Another important aspect of the LVL1 trigger selection strategy presented in this paper is that it will be based only on the topological properties of the events. Our general guiding principle was to try to express the gauge invariance of electromagnetic interactions – which determines the basic properties of the signal events – in terms of topological variables. Such variables assure a robust event selection, fairly insensitive to the time-dependent aspects of the detector and machine operation.

3. Tools and analysis methods

The sample of the lepton-pair signal events was generated with the LPAIR [4] generator. This generator was upgraded to suit our needs (see [1] for details).

⁴In such a scheme, the instantaneous luminosity dependent fraction of the silent bunch crossings must be precisely monitored using a sample of random bunch crossing trigger.

⁵This method uses the minimum bias events to extrapolate the measurement of the absolute luminosity to the “high-luminosity” periods.

For the simulations of the minimum bias events the PYTHIA [5] event generator was chosen. The adequacy of this generator in describing the minimum bias events at the LHC is of secondary importance, for studies presented below. All the efficiencies and acceptances of presented method will be determined directly from the data using large statistics monitoring data samples recorded parasitically over the standard data taking periods. The PYTHIA generator is thus merely used to illustrate the event selection strategy and for the initial specification of the detector and the trigger performance requirements. An underestimation of the background level by a factor of 10 will make the measurement more difficult but will, by no means, invalidate the proposed measurement procedure.

A classical method of optimisation of the detector and the trigger designs should ideally be based on the GEANT [6] simulations of the signal and background events in the fully specified detector. Such a method is, however, of little use for studies requiring a sample of 10^{11} simulated background events. For such a large sample the events, we had to base our studies on simplified methods of tracking of particles in the magnetic field, parametrised simulation of their multiple scattering in the dead material, and an approximate description of the effects of the photon radiation by electrons.

The Coulomb multiple scattering was simulated using a Gaussian approximation [8]. The photon bremsstrahlung in the material was simulated using the Tsai formulae [9]. These simulation simplifications are justified by our aim to determine a safe upper limit of the rate of the background events and the lower limit of the rate of the luminosity signal events. For such a goal the developed tools are both adequate and sufficiently precise.

4. Detector geometry

The geometry of the proposed luminosity detector is shown in Fig. 1. The detector fiducial volume consist of two identical cylinders placed symmetrically with respect to the interaction point. The cylinder has the inner radius of 48 cm, the outer radius of 106 cm and the length 54.3 cm extending from $z_f = 284.9$ cm to $z_r = 339.2$ cm along the beam line. Each cylinder is assumed to have three active layers (the z_1, z_2, z_3 planes) delivering the measurement of the position of a hit left by a particle. These planes are positioned at the distances of $z_1 = 285.8$, $z_2 = 312.05$ and $z_3 = 338.3$ cm away from the interaction point.

The momentum spectrum and the multiplicity of the charged particles traversing the above defined fiducial volume depend upon the magnetic field in which the charged particles propagate. In the studies presented in this paper two field strengths were considered: $B = 0$ T and $B = 2$ T of a uniform, solenoidal magnetic field, labelled respectively as the **B0** and **B2** configurations⁶.

A charged particle entering the fiducial volume of the luminosity detector by crossing the z_1 plane and leaving it by crossing the z_3 plane will be called hereafter the “tagged particle”. Its hits in the detector planes define the luminosity detector “track segment”. The lepton pair production candidate events are identified by the presence of the two tagged particles in the $z > 0$ part of the detector volume and no tagged particles in the

⁶These two configurations correspond to the nominal and the “zero-current” configuration of the ATLAS central tracker solenoid.

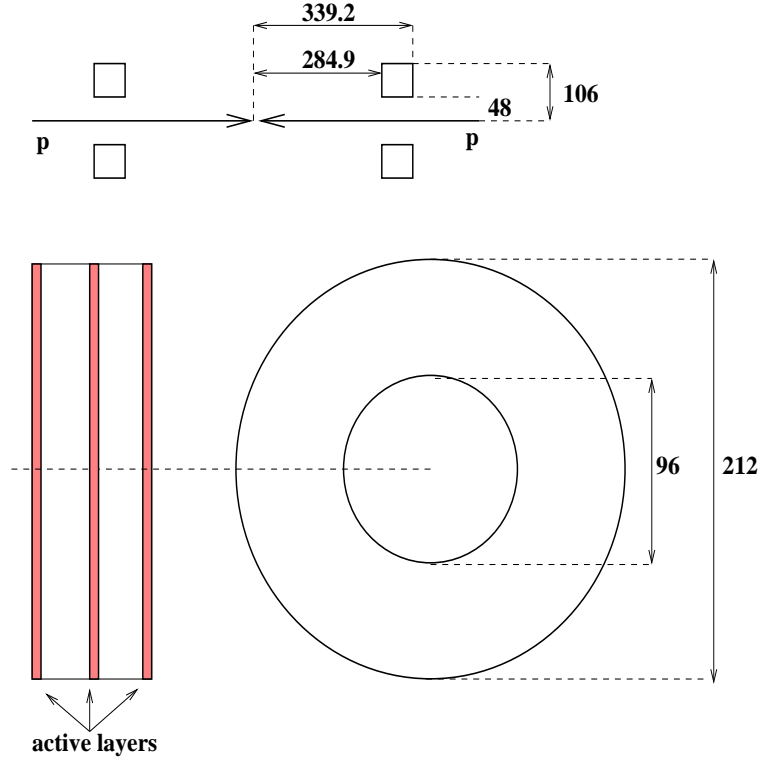


Figure 1. The luminosity detector fiducial volume. Distances are given in centimetres

$z < 0$ part, or equivalently by a mirror reflection of such a configuration. They will be denoted in the following as the “2+0” events. Both, the electromagnetic and the strong interactions of the beam particles may produce “2+0” event signatures.

5. Signal and background events

The strong interaction induced collisions of protons, in particular the diffractive ones, contribute overwhelmingly to the “2+0” event sample. Both, the rates of silent bunch crossings and that of the “2+0” events depend upon the bunch-bunch collision luminosity. For the canonical operation of the LHC machine [7] with 25 ns bunch spacing and at the highest achievable luminosities several proton-proton collisions may take place within one bunch crossing. It was found, using the PYTHIA simulated events, that the probability of two or more proton-proton collisions giving rise to a “2+0” signature is 0.02. Consequently, 98% of bunch crossings with the “2+0” signature have precisely one proton-proton collision. This observation allows us to simplify the background studies by considering the single proton-proton collision events as the dominant background source. All bunch crossings with two or more hadron interaction will be neglected in the estimation of the hadron background to the “2+0” event sample. As a consequence, in the following, the term “2+0” event sample becomes synonymous to the term “2+0” bunch crossing sample.

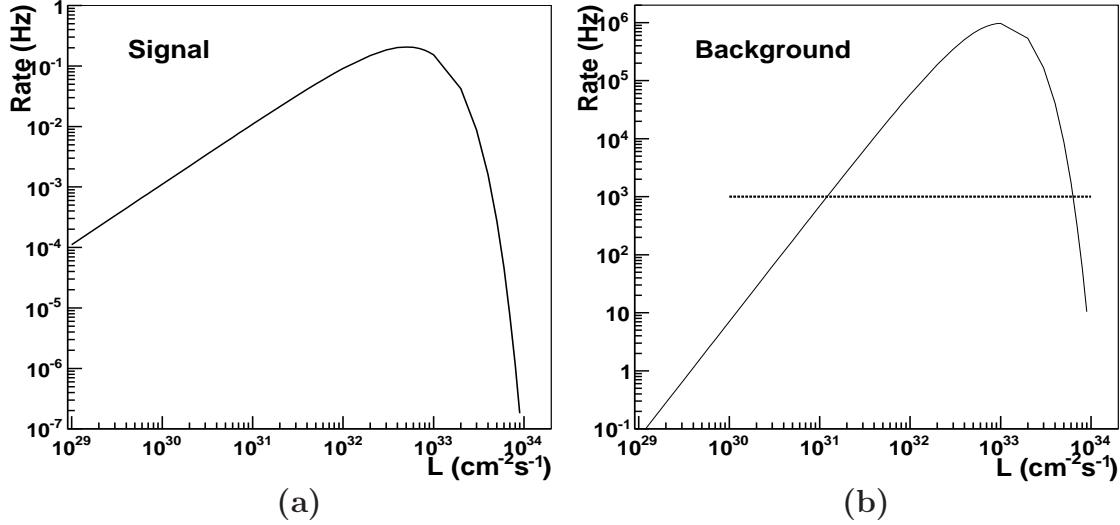


Figure 2. The rate “2+0” events as a function of the machine luminosity: (a) – LPAIR signal events, (b) – PYTHIA background events.

In Figure 2 the machine luminosity dependent rate of the “2+0” bunch crossings for a uniform bunch-by-bunch luminosity distribution and for the 25 ns bunch spacing is presented. Figure 2a shows the rate of the LPAIR signal events. The rate of the PYTHIA hadron background events is depicted in Fig. 2b. The rate of the signal events reaches its maximum of 0.1 Hz at the luminosity of $L = 0.7 \cdot 10^{33} \text{ cm}^{-2} \text{ s}^{-1}$ and decreases rapidly for the luminosity $L \geq 3 \cdot 10^{33} \text{ cm}^{-2} \text{ s}^{-1}$ as the average number of the proton-proton collisions per bunch crossing increases and the probability of the silent bunch crossing decreases. The rate of the background events reaches the level of 700 kHz at the luminosity $L \approx 10^{33} \text{ cm}^{-2} \text{ s}^{-1}$ and decreases rapidly at higher luminosity values for the same reasons. Figure 2a illustrates the instantaneous luminosity range over which a requisite statistical precision of the absolute luminosity measurement can be achieved, for a given data collection time interval. As an example, for the data collected over one year the expected statistical precision is better than 1% for the luminosity range $3 \cdot 10^{30} \leq L \leq 3 \cdot 10^{33} \text{ cm}^{-2} \text{ s}^{-1}$. Figure 2b defines the performance target for the luminosity detector LVL1 trigger. If one assumes 1 kHz input rate as the rate upper limit, which will be allocated by the host detector for the luminosity detector LVL1 triggers, an additional rejection factor of up to 700, must to be achieved.

5.1. Characteristics of the signal and background events

In Figures 3a and 3b the distributions of the momentum, p , and of the transverse momentum, p_T , for the tagged particles in the “2+0” events are shown for the **B2** configuration for the signal and background events, respectively. Two important observations are noted. Firstly, the momenta of the tagged particles are determined by the Lorentz boost which, in turn, reflects the z position of the luminosity detector fiducial volume.

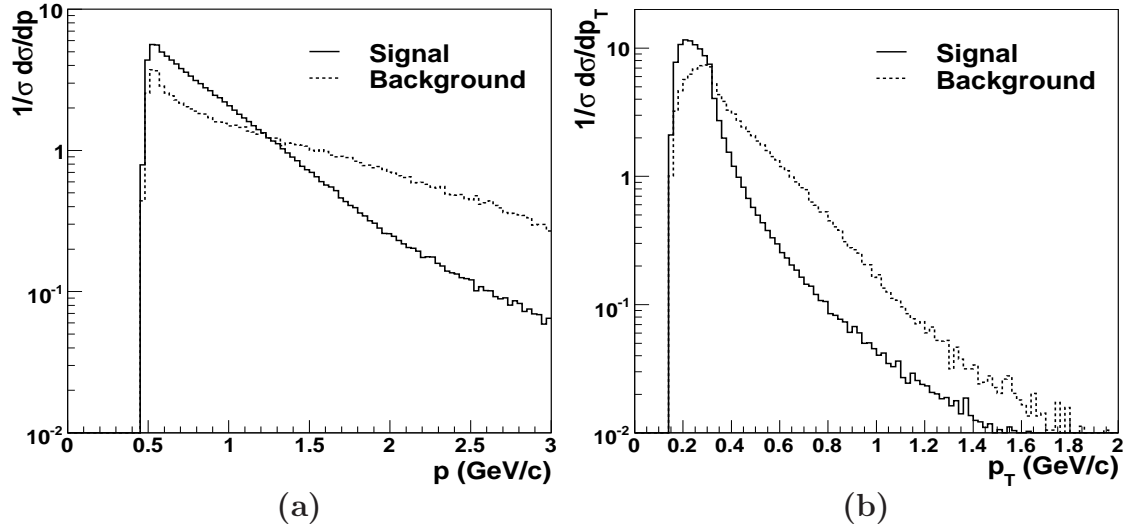


Figure 3. The distributions of: (a) – the charged particle momentum, (b) – the charged particle transverse momentum for the LPAIR signal (the solid line) and the PYTHIA background (the dotted line) “2+0” events for the **B2** field configuration.

Secondly, both the p and p_T distributions are driven solely by the fiducial volume geometry and by the magnetic field strength. Consequently, the acceptance for the tagged particles will be nearly time-independent⁷. It is important to note that the low transverse momentum particles will never reach radially the fiducial volume for the **B2** configuration.

In Figures 4a and 4b the distributions of the transverse momentum, $p_{T,pair} = |\vec{p}_{T,1} + \vec{p}_{T,2}|$, of the two unlike charge tagged particles, and their invariant mass, m_{pair} , for the “2+0” signal and background events are presented. The behaviour of $p_{T,pair}$ distribution in the limit of decreasing transverse momentum is different for the signal and the background samples. For the latter it decreases, as expected, to zero with decreasing $p_{T,pair}$ value while for the signal sample it peaks at small values of $p_{T,pair}$. This behaviour reflects the dominance of the point-like, electromagnetic coupling of protons to the virtual photons for the selected event sample (c.f. [1] for a more detailed discussion of these aspects). The $p_{T,pair}$ variable could thus be used to select efficiently the signal events. Unfortunately, the requisite precision of the $p_{T,pair}$ reconstruction cannot be achieved within the LVL1 trigger latency and its use has to be postponed to the subsequent HLT stages of the data selection procedure.

The distribution of the invariant mass of the pair of tagged particles reflects the corresponding distribution of the pair transverse momentum. The back-to-back pairs have, in general, larger masses for the same momentum spectrum of each of the tagged particles. Note the presence of the hadron resonances (for example $f_2(1270)$) and of the baryon-antibaryon pairs (in the vicinity of 2 GeV) in the invariant mass distribution for

⁷Its time variation will be driven only by the evolution of the length of the proton bunches during the LHC luminosity run (the distributions shown in Figure 3 correspond to the bunch size of 7.5 cm).

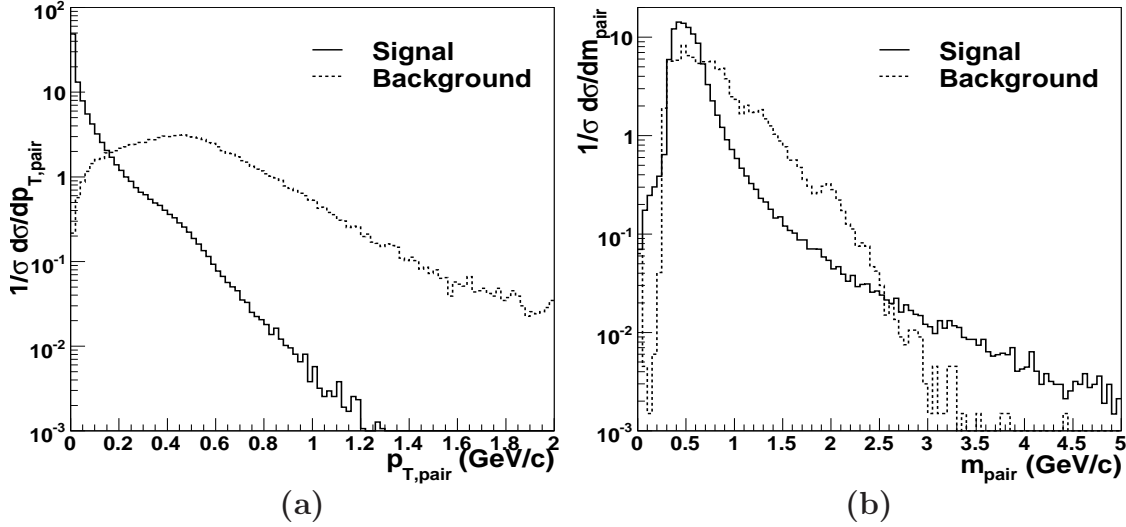


Figure 4. The distributions of: (a) – the transverse momentum, (b) – the invariant mass for the unlike charge particle pairs for the LPAIR signal (the solid line) and the PYTHIA background (the dotted line) “2+0” events for the **B2** field configuration.

the background pairs. Note as well the contribution of the Dalitz decays of neutral pions visible in the region of the smallest invariant masses. The particle type decomposition of the background sources in various mass regions will be crucial for the data driven background subtraction scheme.

The measure of the back-to-back topology of a pair of charged particles is the acoplanarity [1], $\delta\phi$, defined as:

$$\delta\phi = \pi - \min(2\pi - |\phi_1 - \phi_2|, |\phi_1 - \phi_2|)$$

where ϕ_1 and ϕ_2 are the azimuthal angles of the particles at the interaction vertex⁸. The reduced acoplanarity, $\delta\phi_r$, with values between 0 and 1 is defined as $\delta\phi_r = \delta\phi/\pi$.

In Figs. 5a and 5b the distributions of the particle pseudorapidity, $\eta > 0$, and the reduced acoplanarity, $\delta\phi_r$, of the unlike charge tagged particle pairs in “2+0” events are drawn, respectively. A broad η distribution, similar for the signal and the background events, illustrates the effect of the magnetic field which enlarges the acceptance region for particles of the relatively small pseudorapidity. The reduced acoplanarity distribution peaks strongly at $\delta\phi_r \sim 0$ for the signal events. It is approximately flat for the background events. This difference will be of principal importance for the discrimination of the background against the signal by the luminosity detector LVL1 trigger logic. Note, that the flat shape of the reduced acoplanarity distribution for the background events, being insensitive to the details of the modelling of the hadron interactions (it reflects merely

⁸To be precise, the variable defined above describes the acollinearity of the transverse momenta vectors of the particles belonging to a pair. Its name, even if misleading, is retained in our series of papers to follow the convention of the corresponding literature.

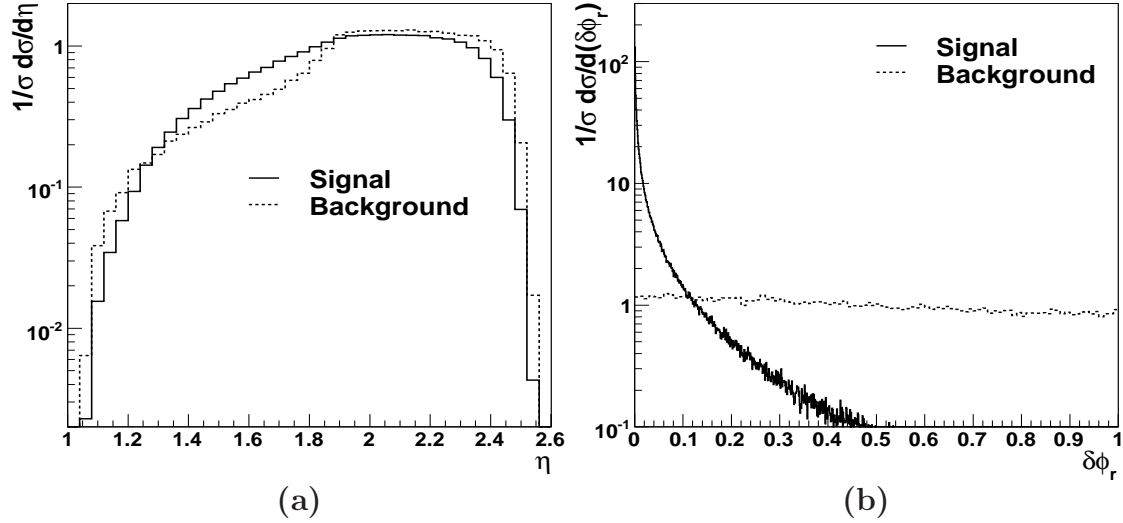


Figure 5. The distributions of: (a) – the charged particles pseudorapidity, η , (b) – the unlike charge particle pair reduced acoplanarity, $\delta\phi_r$, for the LPAIR signal (the solid line) and the PYTHIA background (the dotted line) “2+0” events for the **B2** field configuration.

the longitudinal phase-space), is perfectly suited for a precise, data-based estimation of the background contribution to the signal peak.

An efficient and fast selection of the “2+0” tagged particle configuration and a precise reconstruction of the particle pair acoplanarity will drive the luminosity detector the LVL1 trigger performance requirements discussed in the next section.

6. The detector performance requirements

6.1. Timing resolution

The principal requirement for the timing resolution of the luminosity detector signals is their unambiguous association to the appropriate bunch crossings by the LVL1 trigger logic. Only if this requirement is met the silent bunch crossings can be unambiguously attributed (hence synonymous) to “no-luminosity-detector-signal” bunch crossings⁹.

In our view, a robust bunch crossing association of the detector signals for the **low momentum** tagged particles must be based on the luminosity detector **LVL1 track segment candidates**. The LVL1 timing resolution of the track segments depends both upon the dispersion of the particle flight time before reaching the fiducial volume of the luminosity detector and upon the intrinsic timing resolution of the luminosity detector signals. A robust LVL1 trigger must not only unambiguously assign the track segment signal to a correct bunch crossing but, in addition, it should efficiently reject spurious

⁹Note, that in principle one could use the notion of the “silent-group-of-bunch crossings” if the detector signals cannot be assigned unambiguously to a single bunch crossing. In such a case the applicability domain of the discussed method will be restricted only to the low luminosity machine operation.

beam halo and random detector noise track candidates. In Figures 6a and 6b we show the distributions of the arrival times of the particles at the z_1 and z_3 planes, respectively. The distribution for the tagged particles originating from the bunch-bunch collision vertex is marked with the solid line. The Gaussian distribution of the pp collision time within a bunch crossing of 180 ps was assumed. The distributions of the arrival time at the z_1 and z_3 detector planes for the beam halo particles are plotted with the broken line. It was assumed that the halo particles move in phase (synchronously) with proton bunches. They enter first the z_3 and then the z_1 plane. The tagged particles produced in the bunch-bunch collisions cross the first (third) detector plane delayed by ~ 20 (~ 23) ns with respect to the halo particles associated with the interacting bunch. They arrive to these planes ~ 5 (~ 2) ns before the halo particles associated with the subsequent bunch (for 25 ns bunch crossing spacing). The arrival time distribution for the tagged particles has a significant tail of the “late particles” – specific for the **B2** magnetic field configuration. These “late particles” are characterised by a long helix trajectory.

This study was repeated assuming that the intrinsic detector time resolution of the hits measured in the z_1 and z_3 planes is 0.5 ns. Results of the calculations are presented in Figs. 6c and 6d. These plots demonstrate that the beam halo particles can be efficiently discriminated against the tagged particles originating from the bunch-bunch collision using the measurement of the particle arrival time at the z_1 plane, provided that the intrinsic hit timing resolution is not worse than 0.5 ns. For the z_3 plane position the halo particle hits and the pp collision associated hits cannot be resolved if the machine operates with the 25 ns bunch spacing mode¹⁰.

6.2. Spatial resolution

The discussion presented below is restricted to the requirements for measurement resolution of the azimuthal angle, ϕ , of the hits left by the tagged particles traversing the luminosity detector planes. The angular positions of the hits in the z_1, z_2 and z_3 detector planes will be denoted by ϕ_1, ϕ_2 and ϕ_3 , respectively. A measurement of the radial positions of the hits would certainly be useful in rejecting the spurious track candidates but it is not indispensable for the proposed method. Thus, the radial segmentation of the fiducial volume will not be discussed here.

The presence of the hits in the three detector planes is a minimal necessary condition to detect the interaction-vertex-unconstrained track segments in the case of both the **B2** and the **B0** field configurations. The required ϕ hit resolution in each of the z planes will be determined by the requirement of the reduction of the LVL1 accepted rate of the “2+0” tagged particle pairs to a level of ~ 1 kHz, while retaining a large fraction of the lepton pairs produced in the kinematic region of small acoplanarities.

To quantify the detector resolution requirements we introduce the **coplanar pair selection efficiency** estimator, $\epsilon(\sigma_\phi)$. Its dependence upon the measurement resolution of

¹⁰The precise 0.5 ns resolution timing of the detector signals available for the LVL1 trigger could be of use not only for the luminosity measurement but also for an efficient veto against any high energy halo muons interacting in the detector material and mimicking the missing transverse energy LVL1 signatures. Another important, potential gain from an improvement of the timing resolution is the capacity of a precise discrimination of the proton/kaon/pion track segments. It could be of importance for tagging heavy flavour particles.

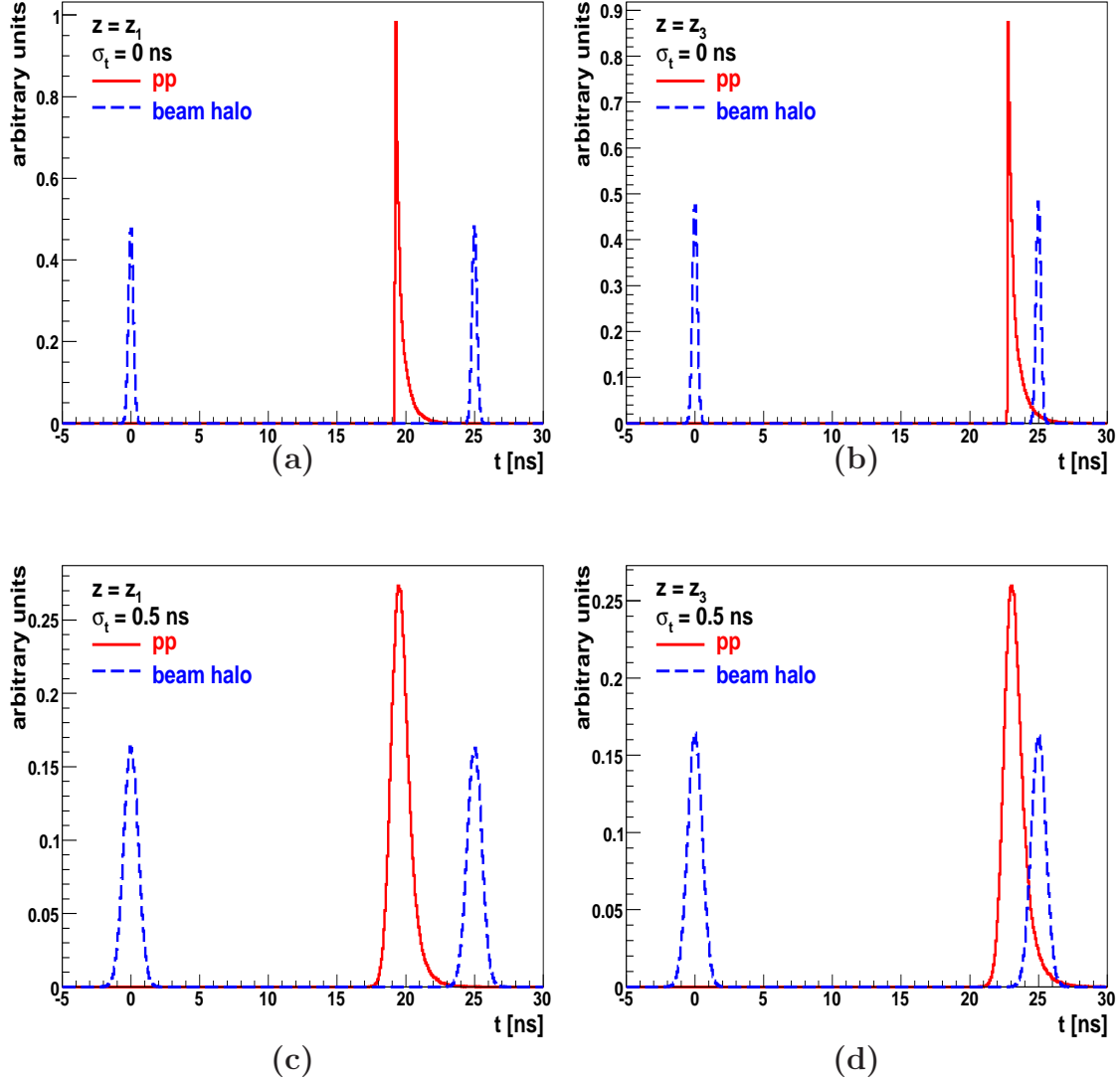


Figure 6. The distributions of the particles' arrival time at: (a) – $z = z_1$, (b) – $z = z_2$ planes. The beam-beam collision vertex originated particles are represented by the full line while the beam halo particles are represented by the dashed line. The relative normalisation of the above two distributions will depend upon the beam conditions and is, at present, arbitrary. The effect of the 0.5 ns Gaussian smearing of arrival-time measurement is shown in plots (c) and (d).

the azimuthal hit position, σ_ϕ , is given by the following formula:

$$\epsilon(\sigma_\phi) = \frac{\int_0^{0.01} f(\delta\phi_r^{rec}, \sigma_\phi) d\delta\phi_r^{rec}}{\int_0^{0.01} f(\delta\phi_r, 0) d\delta\phi_r} \quad (1)$$

where: $\delta\phi_r^{rec}$ is the reconstructed (reduced) pair acoplanarity, and $f(\delta\phi_r, 0)$, $f(\delta\phi_r^{rec}, \sigma_\phi)$ are, respectively, the true and the reconstructed reduced acoplanarity distributions¹¹.

This estimator will be used to map the ‘‘compromise space’’ between the requisite luminosity detector granularity (determining its costs) and the LVL1 trigger capacity for selection of coplanar lepton pairs.

6.2.1. The B_0 field configuration

In the case of the **B0** field configuration the average azimuthal position of the hits in the three detector planes, $\langle \phi \rangle = 1/3 \cdot (\phi_1 + \phi_2 + \phi_3)$, provides the best estimate of the azimuthal angle of the tagged particle and hence, the reconstructed acoplanarity, $\delta\phi_r^{rec}$, of a pair.

In Fig. 7a the $\delta\phi_r^{rec}$ distribution of the lepton pairs for the three values of the detector Gaussian azimuthal resolution, σ_ϕ , is shown. The distribution changes with deteriorating resolution of the detector. For $\sigma_\phi = 0.1$ the characteristic peak at $\delta\phi_r \simeq 0$ disappears due to the migration of events towards the higher acoplanarity values. In Fig. 7b the efficiency, $\epsilon(\sigma_\phi)$, as a function of the azimuthal detector resolution, σ_ϕ is presented. The efficiency was calculated assuming an absence of any detector effects other than the detector resolution. The efficiency drops from value of 1 for a perfect detector to about 0.25 if the particle hit azimuthal resolution is 0.2 radians. For the **B0** field configuration a detector with the azimuthal hit resolution of about 0.03 radians would be sufficient to select the coplanar lepton pair production events with the efficiency better than 0.9 while reducing the hadronic background rate by a factor of about 100.

6.2.2. The B_2 field configuration

In the presence of the solenoidal magnetic field the initial acoplanarity of the small-transverse-momentum lepton pairs will no longer be reflected in the back-to-back topology of the luminosity detector track segments. Their topology depends on the pair invariant mass and rapidity, and on the emission angles of a positively (negatively) charged lepton in the pair rest frame. A multidimensional unfolding of the complete set of lepton pair kinematic variables is fairly complicated and, thus, of little use for efficient LVL1 event selection. The trick proposed here is to directly project the topology of the particles’ hits onto the initial (interaction vertex) pair acoplanarity ignoring the complete reconstruction of the pair kinematics.

In absence of the dead material on the particle path from the interaction vertex to the luminosity detector fiducial volume the charged particles move with a constant azimuthal velocity in the plane perpendicular to the B field, the (x, y) plane, and also with a constant velocity along the B field (the z axis direction). Using cylindrical coordinates the particle

¹¹The restriction of the reduced acoplanarity range is very handy for the detector requirements quantification. The rate of the leptons pairs in this range can be controlled theoretically with a precision better than 1% [1]. The anticipated reduction of the background rate is of the order of a factor 100 due to approximate flatness of the acoplanarity distribution for the background events (c.f. Fig. 5b).

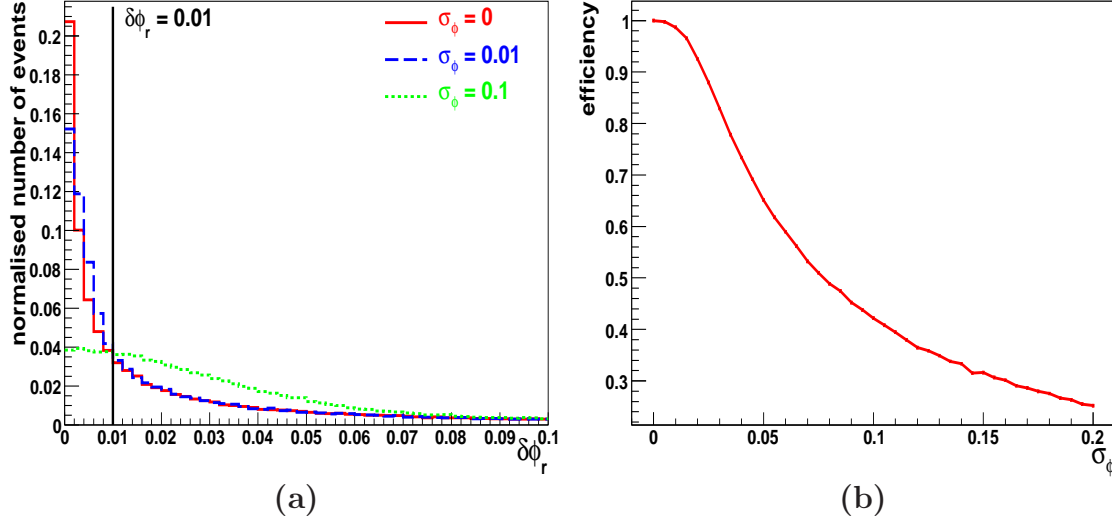


Figure 7. The resolution studies for the B_0 field configuration (LPAIR signal events): (a) – the reduced acoplanarity distribution for the three values of the detector azimuthal resolution, σ_ϕ : 0.0 (the solid line histogram), 0.01 (the dashed line histogram) and 0.1 (the dotted line). (b) – the efficiency, $\epsilon(\sigma_\phi)$ (see text), as a function of the detector azimuthal resolution, σ_ϕ .

azimuthal position, ϕ , evolves with time as:

$$\phi(t) = \phi(z_{vert}) + \omega(B, p_T) \cdot (t - t_{vert}), \quad (2)$$

and its position along the z axis as:

$$z(t) = z_{vert} + v_z(p, p_T) \cdot (t - t_{vert}) \quad (3)$$

where z_{vert} and t_{vert} are the z position of the pair production vertex and the pp collision time, respectively, $\omega(B, p_T)$ denotes the tagged particle angular velocity and $v_z(p, p_T)$ is the z component of the particle velocity.

In absence of the z_{vert} and t_{vert} smearing effects (for “pancake”-like bunches) the pair acoplanarity could, in principle, be determined from the above equations using the measured azimuthal positions of the hits left by the tagged particles. In reality, the $\delta\phi_r$ reconstruction must be done simultaneously with the unfolding of the interaction vertex, z_{vert} , position.

In Fig. 8 the correlation of the interaction vertex longitudinal coordinate, z_{vert} , and the time, t_1 , required for the tagged particle to arrive at the z_1 detector plane is shown. The Gaussian shape of the longitudinal bunch density profile has been assumed with the dispersion of 7.5 cm. At $t = 0$ the interacting bunches fully overlap at $z = 0$ position. Two effects influence the t_1 time for a given vertex position. The first one is the jitter of the collision time determined by the bunch size. It is of the order of 180 ps. The second,

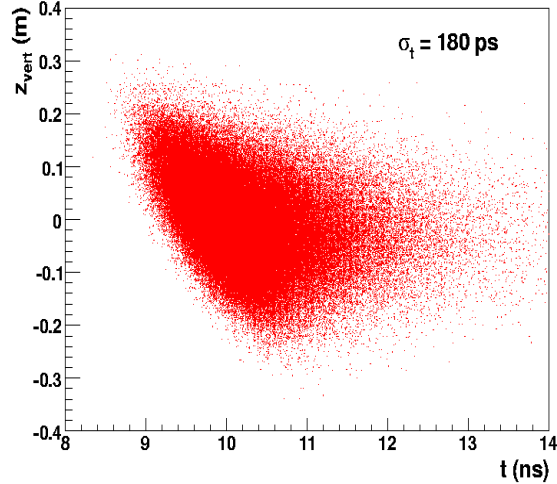


Figure 8. The correlation between the interaction vertex z_{vert} coordinate and the arrival time, t_1 , of the tagged particles (LPAIR signal events) to the detector z_1 plane. The Gaussian bunch density profile with $\sigma = 7.5$ cm has been assumed.

reflects the distribution of the particles' time-of-flight from the production vertex to the z_1 plane. The time-of-flight depends on the particle type, momentum, and its production angle. For the momentum range discussed in this paper the tagged particles move with speed of light along a helix trajectory. Thus the time delay of a hit depend only upon the helix length. Figure 8 shows that the correlation between the particle arrival time and the vertex position z coordinate is weak and that the measurement of t_1 can hardly constrain the vertex position.

A minimal detector requirement to reduce the vertex position uncertainty on the event-by-event basis and, as a consequence, to improve the precision of the initial pair acoplanarity reconstruction, is to measure not only the arrival times of particles at the z_1 plane but also the time-of-flight between the z_1 and z_3 planes.

The equations of motion (2) and (3) written for the two tagged particles have 8 unknown parameters: the interaction vertex z -position, the collision time, the angular and axial velocities and the initial azimuthal angles of each of the two particles. These parameters can be, in principle, unfolded on the pair-by-pair basis from the measured ϕ positions and the relative time of the hits in any two detector planes. However, in reality, the equations of motion along the z axis are quasi-degenerated for the relativistic particles and unrealistic precision of the time measurement would be required to solve this system of equations. Therefore, two approximate reconstruction methods of the z_{vert} vertex position and the reduced (vertex) acoplanarity of a pair are proposed and evaluated in the following.

In the first method the pp collision time jitter is neglected and it is assumed that all collisions take place at $t = 0$. In such a case the z -position of the vertex can be

estimated, for the i^{th} particle using the time of the hits, t_1 and t_3 in the z_1 and the z_3 plane, respectively, as:

$$z_{vert}^i = z_1 - \frac{z_3 - z_1}{t_3^i - t_1^i} \cdot t_1^i. \quad (4)$$

The interaction vertex position is then taken as the average of the positions calculated for each of the tagged particles:

$$z_{est1} = \frac{z_{vert}^1 + z_{vert}^2}{2}. \quad (5)$$

The second method is based on the following measured quantities, for each of the tagged particles denoted by a superscript i :

- the arrival time to the first detector plane, t_1^i ,
- the angular distance, $\Delta\phi_{31}^i = \phi_3^i - \phi_1^i$, of the particle hits in the z_3 and z_1 detector planes,
- the time-of-flight, $t_3^i - t_1^i$ of a particle moving between the z_1 and z_3 planes.

This method simultaneously unfolds the collision time and the position of the vertex under the assumption that the two particles are coplanar (back-to-back in the transverse plane). Such an additional assumption removes the degeneracy of the system of eight linear equations¹². This method provides, thus, a precise estimation of the vertex position for the coplanar pairs. It biases, however, the reconstructed vertex position for the acoplanar pairs. The resulting deterioration of the resolution is regularised by taking the $z = 0$ position for all the pairs for which the estimated collision time is outside the ± 360 ps wide interaction time window. In the following, the vertex position reconstructed with this method will be denoted as z_{est2} .

The above two reconstruction methods are compared, in the following, with a direct method in which no attempt to reconstruct the position of the vertex is made and all pairs are assumed originate from the vertex fixed at $z_{est0} = 0$. In the studies of the relative precision of the above three vertex reconstruction methods it was assumed that the hit-timing in the z_1 plane is measured with a Gaussian resolution of 100 ps while the relative time difference between the hits in the z_1 and z_3 planes is measured with 20 ps accuracy. The calculations were carried out for the 7.5 cm long proton bunches with a Gaussian distribution of their intensities.

Figures 9a and 9b present the correlation between the real and the reconstructed z position of the vertex using the two reconstruction methods, respectively. In Fig. 9c the projections of these scatter plots are compared. The reconstruction precision of the vertex z position determines the reconstruction precision of the azimuthal angles of the particles hence the initial pair $\delta\phi_r^{rec}$. In Fig. 9d the detector resolution dependent efficiency estimators, $\epsilon(\sigma_\phi)$, are compared for the three methods of the vertex z position

¹²Note, that the system of eight linear equation is invariant with respect to ϕ rotation of the reference frame. Therefore, the above six measured quantities and one external constraint is sufficient to reconstruct fully the particle pair kinematics.

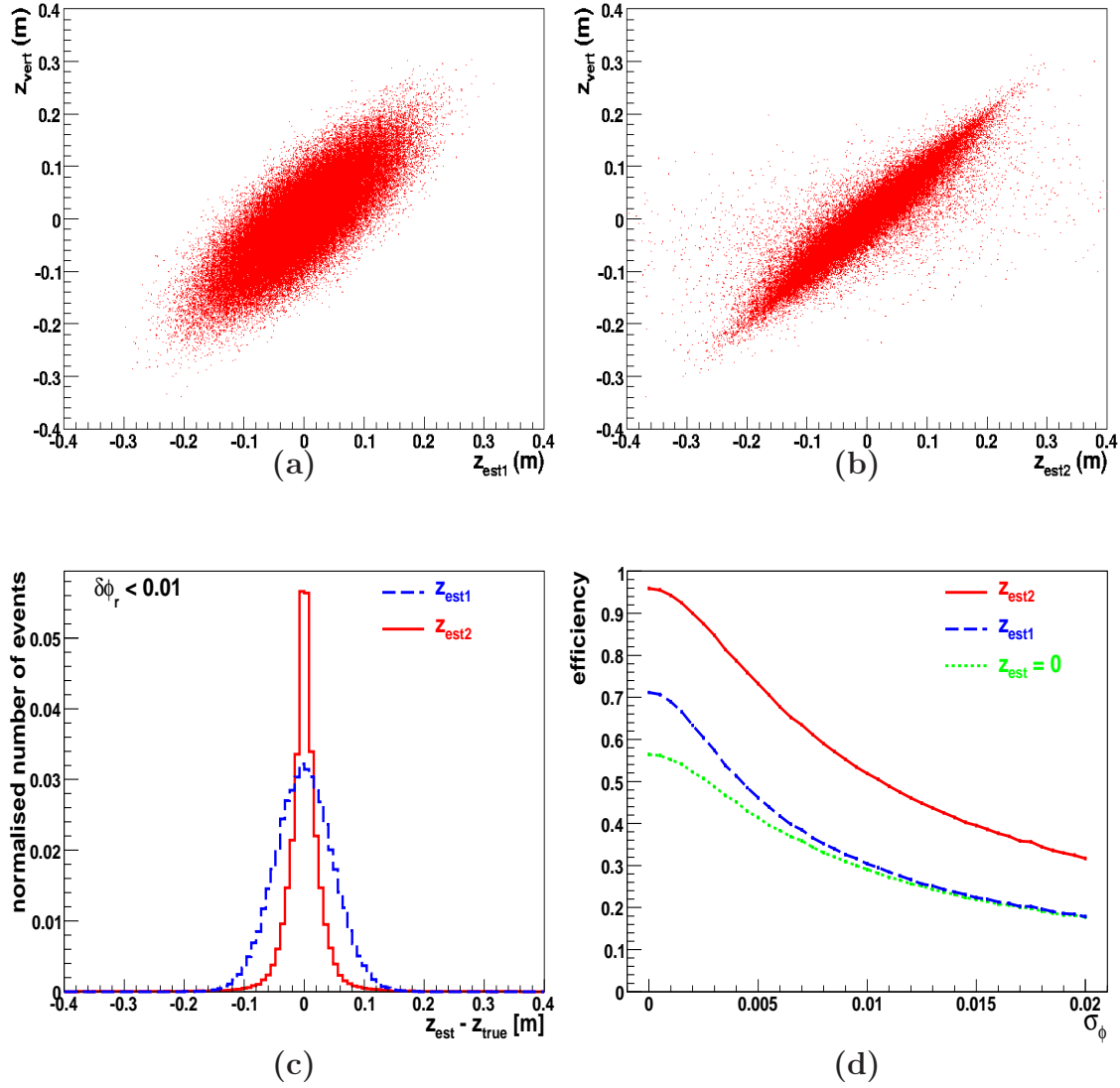


Figure 9. Studies of reconstruction methods of the reduced pair acoplanarity for realistic LHC bunches: (a) – the correlation between the generated, z_{vert} , and the reconstructed, z_{est1} , vertex positions. (b) – the correlation between the generated, z_{vert} , and the reconstructed, z_{est2} vertex positions. (c) – a comparison of the estimated vertex position resolutions for the above two reconstruction methods, (d) – the efficiency, $\epsilon(\sigma_\phi)$, as a function of the detector azimuthal resolution, σ_ϕ , for the three methods of the vertex position reconstruction: $z_{rec} = z_{est0} = 0$ (the dotted line), $z_{rec} = z_{est1}$, (the dashed line), $z_{rec} = z_{est2}$, (the solid line).

reconstruction. If z_{est2} is used, approximately 90% signal pair selection efficiency can be achieved provided that the hits azimuthal position is measured with the accuracy better than 2 mrad. If no hit timing measurement is available and the nominal vertex position is used, the efficiency drops by a factor of about two for the same hit position resolution. The event-by-event reconstruction of the vertex position using the detector timing will be particularly important if the longitudinal emittance of the LHC beams will be worse than that assumed in present studies.

7. The dead material effects

So far an ideal case of particles propagating in vacuum was considered. In reality particles traverse the beam pipe and all the elements of the host detector trackers before reaching the luminosity detector fiducial volume. The effects of multiple scattering and radiation in the corresponding dead material are evaluated in this section.

The studies of the importance of the dead material effects were made for the following three values of the dead material thickness expressed in radiation length units, X_0 : $X/X_0 = 0.2, 0.5, 0.9$. This spread is covering the dead material budget of the ATLAS detector in the relevant η range. The dead material was assumed to be uniformly distributed along the particle trajectory¹³. The luminosity detector z planes were assumed to be $0.1 X_0$ thick.

7.1. Multiple scattering

The Coulomb multiple scattering distorts the charged particle trajectory. Hence, the vertex-extrapolated azimuthal angles of the particles, reconstructed using the luminosity detector track segments may be biased. In Figures 10a and 10b the coplanar pair selection efficiency is plotted for the three radiator thicknesses of 0.2, 0.5 and 0.9 of X_0 as a function of the detector azimuthal angle measurement resolution. In Fig. 10a the efficiency was calculated using the $z_{rec} = 0$ vertex position. This plot demonstrates that multiple scattering does not influence strongly the efficiency dependence upon the detector hit azimuthal resolution. Figure 10b shows the corresponding efficiencies using the reconstructed, $z_{rec} = z_{est2}$, position of the interaction vertex. For the maximal dead material budget the efficiency reaches 80%, in the case of a perfect detector and drops to about 30% for the hit resolution of $\sigma_\phi = 0.02$ radians.

Since the Coulomb multiple scattering distorts predominantly the low momentum particle tracks its effects can be reduced further by restricting our sample to high momentum particles. A luminosity detector estimator of the particle momentum, which can be directly used by the luminosity detector LVL1 trigger logic, is the angular distance of particle hits in the third and in the first detector plane, $\Delta\phi_{31}^i = \phi_3^i - \phi_1^i$. Its correlation with particle momentum is illustrated in Fig. 11a where the distribution of the particle momentum distribution is shown for the three different cuts on $\Delta\phi_{31}$: *no cut*, $\Delta\phi_{31} < 15^\circ$ and $\Delta\phi_{31} < 10^\circ$. In the case of $\Delta\phi_{31} < 15^\circ$ only particles of momenta $p_{tot} > 0.6$ GeV/c are accepted, while the requirement of $\Delta\phi_{31} < 10^\circ$ cut-off moves this limit to almost

¹³This rather crude approximation of the reality is sufficiently precise for the studies presented in this paper. In the real experimental analysis the distribution of the dead material will be determined precisely using the gamma ray conversion tomography of the host detector tracker.

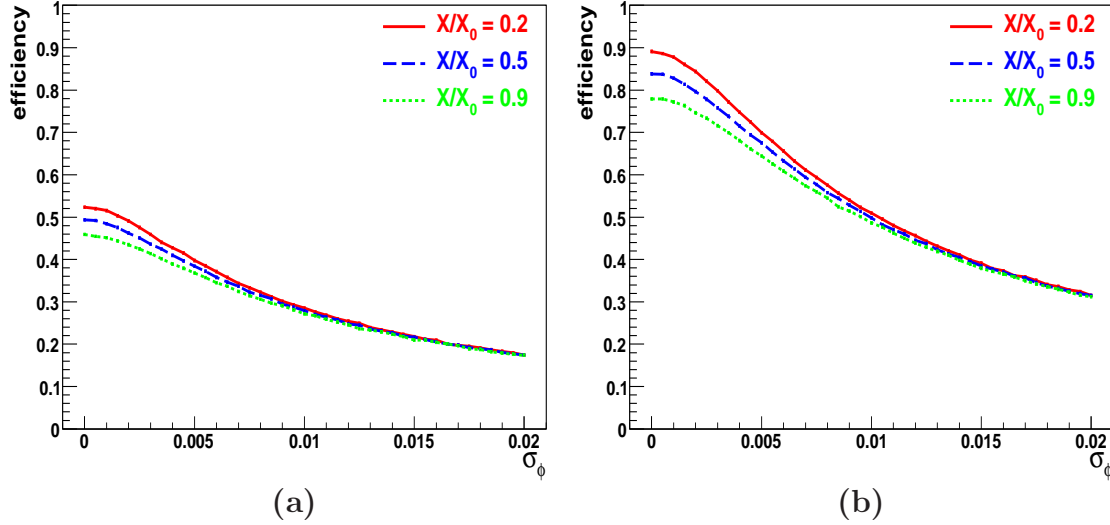


Figure 10. Coulomb multiple scattering studies (LPAIR signal events): (a) – the coplanar pair selection efficiency as a function of the detector azimuthal resolution for the three dead material thicknesses expressed in radiation length units, of: 0.2 (the solid line), 0.5 (the dashed line), 0.9 (the dotted line) for the reconstructed vertex position, $z_{rec} = 0$, (b) – as before, but for the reconstructed position of the interaction vertex position, $z_{rec} = z_{est2}$.

1 GeV/c.

The efficiencies calculated for the above three subsamples of events, for $z_{rec} = 0$, are compared in Fig. 11b. As can be observed the efficiency increases with decreasing value of the cut on $\Delta\phi_{31}$ and for a perfect detector it changes between 45% and 65% for the $\Delta\phi_{31}$ cut-off value ranging from *no-cut* to 10° . The efficiency decreases with deteriorating azimuthal resolution and reaches about 20% for $\sigma_\phi = 0.02$ radians irrespectively of the $\Delta\phi_{31}$ cut value. The effective particle momentum cut reduces not only the impact of the multiple scattering effects on the coplanar pair selection efficiency. It reduces as well the sensitivity of the selection efficiency to the reconstruction precision of the collision vertex position.

7.2. Radiation

The effects of multiple scattering concerns both the e^+e^- and the $\mu^+\mu^-$ pairs. In this section the radiation effects are evaluated. These effects are of importance only for the e^+e^- pairs.

The radiation of photons leads to the electron energy losses in the dead material. Overwhelming majority of photons are emitted co-linearly to the electron trajectory. In the absence of magnetic field the electron azimuthal angle is unchanged by the photon emission and the reconstructed pair acoplanarity remains unaffected.

In the presence of magnetic field this is no longer the case, in particular for catastrophic losses of the electron energy associated with radiation of hard photons.

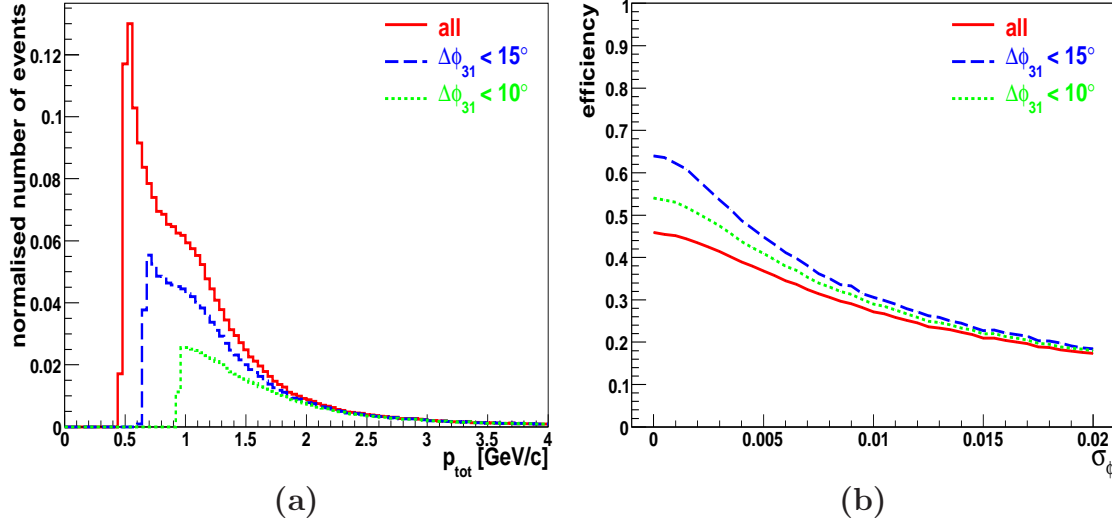


Figure 11. The effective particle momentum cut-off and its effect on the efficiency of the coplanar pair selection in the presence of the Coulomb multiple scattering effects (LPAIR signal events): (a) – the particle momentum distribution for the full sample tracks (the solid line) and for a subsample of tracks satisfying the following two constraints: $\Delta\phi_{31} < 10^\circ$ (the dotted line) and $\Delta\phi_{31} < 15^\circ$ (the dashed line), (b)– efficiency, $\epsilon(\sigma_\phi)$, as a function of the detector azimuthal resolution for the three values of $\Delta\phi_{31}$ cut: no cut (the full line), $\Delta\phi_{31} < 10^\circ$ (the dotted line) $\Delta\phi_{31} < 15^\circ$ (the dashed line), the $z_{\text{rec}} = 0$ was assumed.

The radiation gives a rise to the following two effects. Firstly, the electrons produced in the acceptance region of the luminosity detector may no longer reach its fiducial volume. Secondly, even, if they reach its fiducial volume their angular velocities, $\omega(B, p_T)$ will be different from the initial ones. Consequently, the extrapolated pair acoplanarity could deviate significantly from the true, initial one. Both effects reduce the coplanar pair selection efficiency.

In Fig. 12a the distributions of the initial reduced acoplanarity of the electron pairs are shown for four different radiator thicknesses. These distributions are sensitive to the dead material distribution on the path of particles from the production vertex up to the luminosity detector fiducial volume. The largest impact is due to the dead material in the vicinity of the collision vertex, because it influences a large fraction of the particle path. The distributions shown in Fig. 12a were obtained assuming that the radiator is placed at the collision vertex¹⁴. They represent, thus, the maximal losses of the signal pairs.

Figure 12b shows the efficiencies, $\epsilon(\sigma_\phi)$, as a function of the detector azimuthal resolution for the four values of the radiator thickness. The function drawn with the solid line represents the ultimate efficiency function for the zero thickness of the radiator. The radiator presence leads to lower efficiency values. In the case of $0.9 X_0$ thick radiator the

¹⁴Precise simulations including the realistic dead material distribution are beyond the scope of this paper.

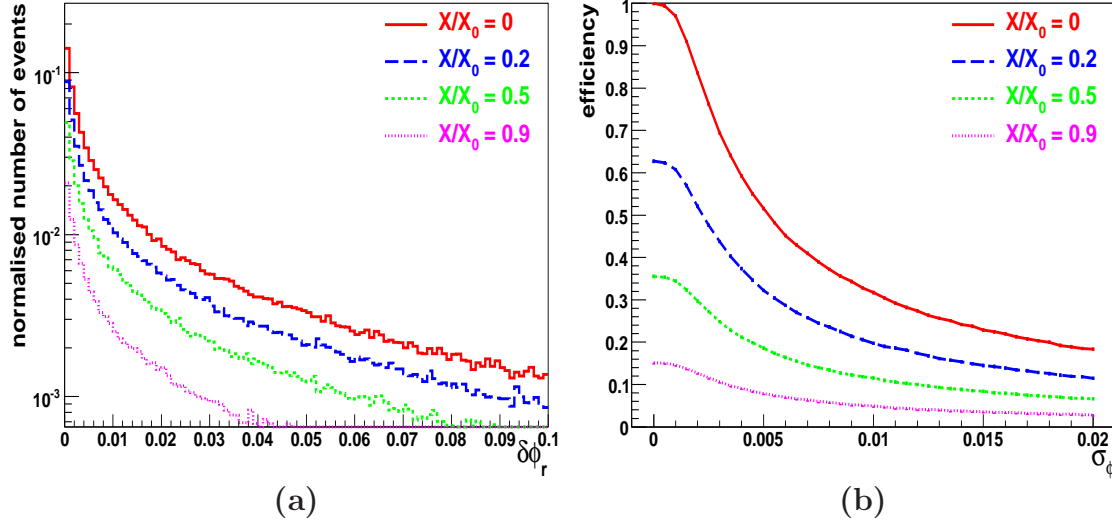


Figure 12. The study of the radiation effects on the coplanar lepton pair selection efficiency: (a) – the reduced acoplanarity distribution at the interaction vertex for the four thicknesses of the dead material in units of X_0 : 0 (the solid line), 0.2 (the dashed line), 0.5 (the dotted line), 0.9 (the dash-dotted line), (b) – the coplanar pair efficiency, $\epsilon(\sigma_\phi)$ as a function of the detector azimuthal resolution, for the above four thicknesses of the dead material.

perfect detector efficiency drops to about 15% and its value is reduced to 5% for $\sigma_\phi = 0.02$ radians.

7.3. Multiple scattering and radiation

The coplanar pair selection efficiencies, $\epsilon(\sigma_\phi)$, plotted as a function of the detector azimuthal resolution, for the three values of the dead material thickness, and for the **B0** field configuration, are presented in Fig. 13a. The pair acoplanarity was reconstructed from the average azimuthal positions of the hits left by the leptons in the detector layers. The efficiency is high and depends weakly on the detector azimuthal resolution. If the radiator is $0.9 X_0$ thick the efficiency is about 70% and practically does not depend on the detector ϕ measurement resolution. This figure demonstrates that in absence of the detector magnetic field:

- the extrapolation of tagged tracks to a common vertex is not indispensable to determine their initial acoplanarity,
- the measurements are largely insensitive to the photon radiation effects,
- the effects of multiple scattering is more pronounced than in the case of the **B2** field configuration (small momentum particles are no longer swept out by the magnetic field)

- the coplanar lepton pairs can be efficiently selected by the luminosity detector even if its azimuthal angle measurement resolution is very modest.

The presented efficiencies are the same for the e^+e^- and the $\mu^+\mu^-$ pairs. This is no longer the case for the **B2** field configuration.

The efficiencies modified by the multiple scattering and radiation effects, for the **B2** field configuration are presented in Figure 13b. Again, the efficiency, $\epsilon(\sigma_\phi)$, is shown as a function of the detector azimuthal angle measurement resolution. All distributions correspond to the maximal dead material budget, $X/X_o = 0.9$, and to the worst case of the dead material concentrated in the vicinity of the interaction vertex.

The solid line represents to the coplanar pair selection efficiency for the $\mu^+\mu^-$ pairs for the luminosity detector capable to measure both the azimuthal position of the tagged particle hits and their timing. We recall that these measurements allow for a precise reconstruction of the position of the interaction vertex: $z_{rec} = z_{est2}$. The efficiency reaches 80% and drops to about 55% for $\sigma_\phi = 0.02$. The dashed line shows the efficiency for the $\mu^+\mu^-$ pairs for a detector which does not provide the timing measurement of the particle hits. In this case, the event-by-event reconstruction of the vertex position cannot be made and its nominal position, $z_{rec} = 0$, is assumed for each of the observed pairs. The efficiency reaches 46% for an ultimate precision detector and drops to about 20% for $\sigma_\phi = 0.02$. The dotted line shows the efficiency for the e^+e^- pairs for a detector which does not provide the timing measurement of the tagged particle hits. Again, the nominal position $z_{rec} = 0$ value for each of the observed pairs is assumed. The drop of efficiency is driven basically by the radiative processes. The efficiency reaches 8% for an ultimate precision detector and drops to about 4% for $\sigma_\phi = 0.02$.

Studies presented in this section points out to the three emerging methods of the luminosity measurement. Each of them puts different emphasis on different performance aspects of the luminosity detector. For the measurement using muon pairs a precise hit timing measurement and a high azimuthal granularity of the luminosity detector are crucial to achieve the highest possible selection efficiency of coplanar pair selection. This is important because only small fraction of large momentum muons will be able reach the muon spectrometer and be subsequently identified and selected by the LVL2 and the EF triggers of the host detector¹⁵. For the measurement using e^+e^- pairs the detector timing functions and its fine ϕ -granularity are less important because the coplanar pair selection efficiency is driven mainly by the electron radiation in the dead material of the host detector. The same conclusion can be made for the luminosity measurement in the **B0**-periods of the host detector operation, even if for totally different reasons. It is important to note that the high coplanar pair selection efficiency in the **B0** periods allows to achieve a comparable statistical precision of the luminosity measurement in about ten times shorter time intervals, than in the case of the **B2** periods.

¹⁵Note that the position of the luminosity detector at the η -extremity of the host detector tracker maximises muon total momentum for a fixed transverse momentum value.

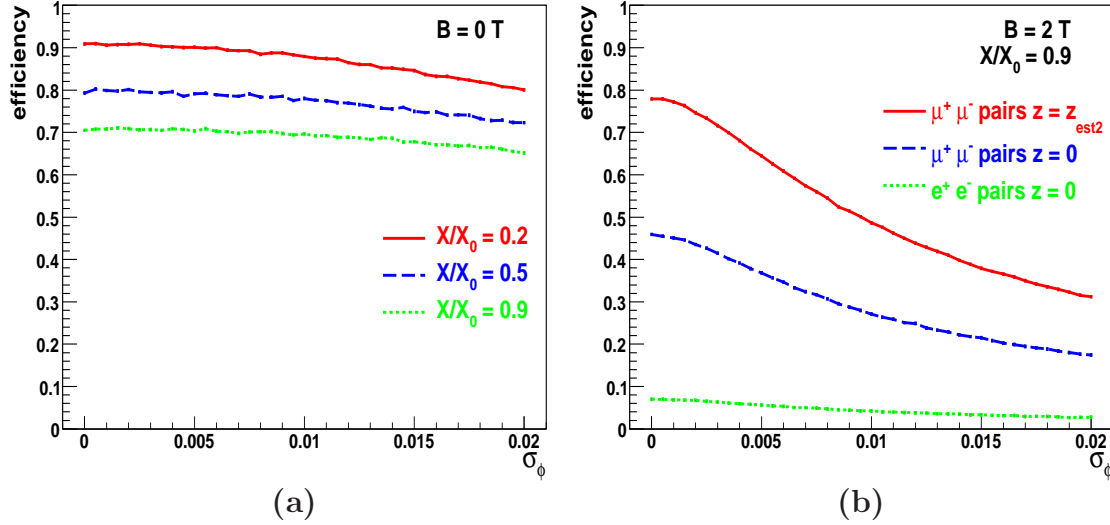


Figure 13. The efficiency, $\epsilon(\sigma_\phi)$, as a function of the detector azimuthal resolution, σ_ϕ : (a) – for the $B0$ field configuration, and for the three values of the dead material thickness expressed in the radiation length units: 0.2, 0.5 and 0.9 (the dashed, the dotted and the dash-dotted lines, respectively), (b) – for the $B2$ field configuration and for the dead material thickness of 0.9. The solid and the dashed lines, for the opposite charge muon pairs, correspond to, respectively, the $z_{rec} = z_{est2}$ and $z_{rec} = 0$ values. The dotted line, for the electron-positron pairs, correspond to $z_{rec} = 0$ value.

8. The trigger and the data acquisition system requirements

8.1. Operation aspects

In previous sections the timing and the space resolution requirements for the luminosity detector were discussed. They were driven basically by its capacity to select coplanar lepton pairs with the highest achievable efficiency. These requirements have to be complemented by the requirements that the coplanar lepton pairs must be selected within the host detector LVL1 latency time and that the selection process must be monitored with adequate precision. These above two requirements will determine the trigger and the data acquisition performance requirements discussed in this section.

Ideally, for a noiseless detector and for perfectly collimated beams the silent bunch crossings could be identified by the LVL1 trigger logic of the luminosity detector by demanding zero multiplicity of the track segments both in the left and in the right arm of the luminosity detector. Event candidates for the luminosity measurement could be identified by the LVL1 trigger logic as those with two track segments in the left (right) arm of the luminosity detector and no track segment in the other arm. This LVL1 sample of preselected events would be still dominated by the "non-silent" bunch crossings, in which the luminosity detector signals are due to hadrons produced in diffractive strong interaction collisions. However, by demanding that the vertex extrapolated pair acoplanarity

satisfies the condition: $\delta\phi_r < 0.01$ the rate of these background events can be reduced, using solely the luminosity detector data, to the level of few kHz in a wide range of the machine luminosities. This rate, could be reduced further by the Central Trigger Processor (CTP) of the host detector, by using the full set of the host detector LVL1 trigger bits. The corresponding reduction factor could be dynamically adjusted to the allocated share of the host detector trigger and data acquisition capacities such that the LVL1 accepted luminosity events represent a "non-interfering" fraction of the host detector LVL1 accepted events.

In the LVL1-selected luminosity event candidates sample, the hadron background events outnumber the l^+l^- signal events still by a factor of $\mathcal{O}(10^5)$. Their rate could be reduced to a signal event rate of $\mathcal{O}(0.1 \text{ Hz})$ using the present capacity of the HLT system of the host detector. At such a small rate, recording the full host and luminosity detector information by the host detector Data Acquisition (DAC) system would hardly interfere with the host detector canonical operation modes.

The final sample of the HLT selected luminosity event candidates would be populated mostly the peripheral electromagnetic collision events in which a coplanar lepton pair is produced. Their final analysis could be done off-line concurrently with the analysis of any user defined subsample of events providing the absolute normalisation of the measured cross section independently of the data quality criteria.

In reality, the luminosity detector operating conditions may be different from the ideal ones and varying with time, instantaneous bunch-by-bunch luminosity, beam currents, β^* , the beam crossing angle and with other parameters. In addition, the detector may have the periods of noise producing spurious track segments. Therefore, the luminosity detector LVL1 trigger algorithm must be able to identify the coplanar pairs in the bunch crossings where several track segments, not associated with beam-beam collisions, are observed in each of the luminosity detector arms. Since the algorithm processing time increases with the square of the number of track segments this remedy has a sharp processing power dependent limit.

For a scheme to be robust against any variation of the data taking conditions, supplementary "rate-stabilising" methods are required. The first one, protecting the triggering scheme against beam halo track candidates is to validate the track segments with the precise time stamps. As discussed earlier this requires the hits in the z_1 plane to be measured with 0.5 ns resolution. In the periods of large machine noise the search for coplanar lepton pairs could be made using track segments with the beam-beam interaction window time stamp.

Another protection against periods with large number of spurious track segments would be to use in the searches of coplanar pairs only those of the track segments which are likely to be left by the electrons. This remedy would require either a dedicated luminosity detector technology or an extension of the present object-multiplicity driven LVL1 logic of the host detector CTP to a scheme in which the topological association of the trigger elements is made. These aspects are beyond the scope of this series of papers and will not be discussed here.

8.2. Monitoring aspects

In order to achieve the luminosity measurement precision target the event selection process will have to be precisely monitored and the event selection efficiency, and acceptances are required to be determined directly from the data. In addition, the background subtraction scheme is required to be independent of the modelling precision of the strong interactions of the colliding protons. Those criteria drive the principal performance requirements for the DAQ system of the luminosity detector and constrain its incorporation within the DAQ system of the host detector.

Fulfilling these requirements is facilitated in the proposed scheme in which the luminosity detector is embedded within the fiducial volume of the tracker of the host detector. As discussed earlier, owing to such a configuration all the particles crossing the luminosity detector will have their tracks reconstructed and the energy deposits measured by the host detector. This will allow to use a large sample of reconstructed minimum bias events, associated parasitically with any type of selected events, for the data driven background subtraction and for the data-driven determination of the event selection efficiencies. Owing to a large statistics of such events, the particle identification capacity of the host detector, and the use of the hadron resonances as the tagged sources of the all the particle species, the lepton pair selection efficiencies and the hadron background can be precisely controlled on the bunch-by-bunch basis in a wide range of the instantaneous luminosities.

The principal requirements are thus confined merely to the performance aspects of the DAQ system of the luminosity detector, in particular to its efficiency in collecting of the dedicated samples of the monitoring events.

For example, it is required that the number of validated "in-time" and "out-of-time" track segments in the ϕ -sectors of the luminosity detector is monitored by the local data acquisition system to provide a very fast, bunch-by-bunch relative luminosity determination. The DAQ system of the luminosity detector must provide a precise monitoring of the time evolution of the rate of the silent bunch crossing both for each of the interacting and the pilot (those which do not have bunch partners to collide) bunches. To achieve this goal the silent bunch crossings will have to be monitored locally, and controlled globally using random events collected by the host detector.

9. Conclusions and outlook

In our previous paper [1], the phase-space region of the lepton pair production process $pp \rightarrow l^+l^- + X$ was selected. We have shown that its rate can be theoretically controlled at the LHC to a $\leq 1\%$ precision. In the present paper a realistic proposal of the selection strategy of a significant fraction of events produced in this region was presented.

The main obstacle for the present LHC detectors to implement such a scheme is a missing capacity of their LVL1 trigger to reduce by seven orders of magnitude the rate of the background hadron pairs produced in ordinary strong interaction mediated collisions of the beam particles.

A remedy proposed in this paper is based on two ideas. The first one is to select already by the LVL1 trigger only events with back-to-back pairs, leaving the lepton identification to the subsequent event selection stages. The second one is to drastically reduce the

number of bunch crossings in which coplanar pairs are searched to the subsample of "silent bunch crossings" and monitor their frequency using the random bunch-crossing trigger.

Their implementation requires an upgrade of one of the LHC detectors by incorporating within its fiducial volume a dedicated "luminosity detector". Its main goal is to analyse, within the LVL1 trigger latency, the topology and the origin of the particle hits detected in its fiducial volume, and to deliver the LVL1 accept/reject signal to the CTP unit of the host detector.

The minimal requirements for the timing and for the spacial hits- resolutions were analysed in a realistic operation environment, including a finite-size particle bunches and the effects due to dead material. It was demonstrated that for a very modest detector resolution requirements the lepton pair candidate events can be efficiently selected.

An implementation of the proposed scheme based on a concrete model of the luminosity detector LVL1 trigger and including a complete, host detector signal based, LVL2 trigger and Event Filter selection procedure of the luminosity events will be presented in the forthcoming paper.

REFERENCES

1. M. W. Krasny, J. Chwastowski and K. Słowikowski, Nucl. Instrum. Meth. **A584** (2008) 42.
2. The ATLAS Collab., G. Aad et al., J. Inst. **3** (2008) S08003.
3. ATLAS Collab. CERN-LHCC-2003-022.
4. S. P. Baranov, O. Dunger, H. Shooshtari and J. A. M. Vermaseren, Proc. of Physics at HERA, vol. 3, (1992) 1478.
5. T. Sjöstrand, P. Edén, C. Friberg, L. Lönnblad, G. Miu, S. Mrenna and E. Norrbin, Computer Phys. Commun. **135** (2001) 238.
6. R. Brun et al., Geant 3.21, CERN Program Library Long Writeup W5013, Geant4 Collab., S. Agostinelli et al., Nucl. Instrum. Meth. **A506** (2003) 250, Geant4 Collab., J. Allison et al., IEEE Trans. Nucl. Science **53** (2006) 270.
7. LHC White Book, CERN/AC/93-03, LHC Conceptual Design Report, CERN/AC/96-05.
8. Particle Data Group, C. Amsler et al., Phys. Lett. **B667** (2008) 1.
9. Yung-Su Tsai, Phys. Rev. **149** (1966) 1248, Rev. Mod. Phys. **46** (1974) 815; erratum Rev. Mod. Phys. **49** (1977) 421.